Title
YIELDS AND TRAPPING OF NEUTRAL DEUTERIUM BEAMS CONTAINING 3nu MOLECULES

Permalink
https://escholarship.org/uc/item/4r6074p0

Authors
Berkner, K.H.
Morgan, T.J.
Pyle, R.V.
et al.

Publication Date
1972-08-01

Submitted to Nuclear Fusion

LBL-1026
Preprint

YIELDS AND TRAPPING OF NEUTRAL DEUTERIUM BEAMS CONTAINING $^3\Pi_u$ MOLECULES

K. H. Berkner, T. J. Morgan,
R. V. Pyle, and J. W. Stearns

August 1972

AEC Contract No. W-7405-eng-48

LBL-1026

LBL-1026

YIELDS AND TRAPPING OF NEUTRAL DEUTERIUM BEAMS CONTAINING $^3\Pi_u$ MOLECULES*

K. H. BERKNER, T. J. MORGAN,[†]
R. V. PYLE, J. W. STEARNS

Lawrence Berkeley Laboratory
University of California
Berkeley, California 94720, U. S. A.

August 1972

ABSTRACT

Experimental yields of neutral ground-state atoms and molecules and long-lived $^3\Pi_u$ excited molecules from interactions of 30- to 120-keV D_2^+ ions in magnesium vapor are reported. Results of calculations that approximate trapping in magnetically confined plasmas of beams produced by either D^+ or D_2^+ ions neutralized in Mg vapor are given.

---

[*] Work performed under the auspices of the U. S. Atomic Energy Commission.

[†] Present address: Department of Pure and Applied Physics, Queen's University, Belfast BT7 INN, N. Ireland.

1. INTRODUCTION

The buildup, replenishment, and heating of plasma in a fusion plasma experiment or reactor can be accomplished by injection of beams of electrically neutral particles. Production and destruction probabilities of hydrogen atoms and ground-state molecules are sufficiently well known [1] that the attenuation of beams of these particles can be calculated fairly well [2]. Some preliminary work on penetration of clusters of hundreds of atoms [3] and of macroparticles [4] has also been carried out.

One way to build up an energetic plasma in an initially high-vacuum magnetic trap is by Lorentz ionization of highly excited hydrogen atoms in the $\vec{v} \times \vec{B}$ equivalent electric field [5,6]. Because the atoms typically are produced a meter or more from the trapping region, only atoms with principal quantum numbers $n \gtrsim 6$ have lifetimes sufficiently long to survive. As the plasma density increases a collisionally induced upward cascading of excited states occurs [7], and a density is reached at which the highly excited atoms are ionized at large radii, while the ground-state atoms pass through the plasma with little attenuation.

Several years ago Hiskes noted that beam trapping at intermediate densities could be improved if there were long-lived hydrogen atoms with collisional ionization cross sections larger than that of the ground state, but not so highly excited as to cascade upward and Lorentz ionize [8]. The metastable 2s state would qualify except that it is quenched by passage through weak magnetic fields. Hiskes showed that the hydrogen molecule in the $^3\Pi_u$ state (in the unitedatom approximation this is similar to a hydrogen atom in the n = 2 level) is long lived. By analogy with electron capture by protons, it should be produced efficiently by electron capture at low energies in metal vapors, and therefore is a candidate for neutral injection [9].

We have measured the yields of 30- to 120-keV electronic ground state ($^1\Sigma_g$) and 40- to 80-keV long-lived excited ($^3\Pi_u$) deuterium molecules produced by electron capture in magnesium vapor[1]. The details of the experiment and some relevant cross sections are reported elsewhere [10]. In this paper we give information about experimental yields of $^3\Pi_u$ molecules and other particles that might be obtainable from an injector, and examples of trapping calculations.

2. YIELDS

Experimentally [10], about 36% of the non-dissociative electron capture by 44-keV D_2^+ ions in Mg vapor produces n = 2, $D_2(^3\Pi_u)$ molecules, the proportion dropping to about 23% at 140 keV. More interesting quantities, from a practical standpoint, are the numbers of $^3\Pi_u$ molecules and other neutral species that emerge from the charge-exchange cell per incident D_2^+ ion.

Figures 1 and 2 show as a function of Mg-neutralizer thickness the fractions of an incident D_2^+ beam that emerge from the charge-exchange cell as D_2 molecules in all states, and as D_2 molecules in the $^3\Pi_u$ state. Also shown in Fig. 1 are results obtained by Riviere et al. [11,12]. The total yield of molecules (Fig. 1) includes a small contribution from highly excited hydrogen-like (Rydberg) states with $n \gtrsim 8$ [12,13]. Maximum yields (at optimum target thickness) are summarized in Fig. 3.

The number of atoms per incident D_2^+ ion that emerge from a Mg neutralizer is shown in Fig. 4. At equilibrium, all molecules will have been dissociated, and the yield should approach twice the equilibrium fractions obtained with a primary D^+ beam of the same velocity. These doubled atomic equilibrium fractions are also shown in Fig. 4: The lines marked A are measured fractions of Futch and Moses [14]; the lines marked B are calculated from cross sections reported by Berkner, Pyle, and Stearns [15].

From Figs. 1-4 and Ref. [10] we find, for example, that if 40-keV D_2^+ ions are incident on a Mg-vapor target with a thickness of 10^{15} atoms/cm^2, then approximately 7% of the incident beam power emerges carried by $D_2(^3\Pi_u)$ molecules, 14% by ground-state molecules, 60% by deuterium atoms, 11.5% by D_2^+ ions, and 7.5% by D^+ ions.

As mentioned in Ref. [10], we found no significant $^3\Pi_u$ molecule yields from D_2^+ ions incident on H_2 or N_2 neutralizers (this is consistent with predictions by Hiskes), or from collisional breakup of D_3^+ ions.

3. PLASMA TRAPPING OF INJECTED D AND D_2 BEAMS

In this section we give some examples of the variation of trapping parameters with beam composition. The calculations are not oriented toward any specific experimental plasma device, but rather are intended to give some insight into the effects produced by different beam compositions. In this spirit we consider the trapping that results when neutral beams, prepared by D^+ or D_2^+ passing through a Mg neutralizer, impinge upon a plasma target. For these calculations we consider an incident beam accelerated to 10 keV/nucleon (20 keV D^+ or 40 keV D_2^+).

No attempt has been made to fold in velocity distributions--for collisions of the beam with plasma ions we take the relative velocity to be the beam velocity; for collisions with electrons, we take the relative velocity to be the velocity of electrons with an energy equal to the electron temperature. In the absence of cross-section data for $D_2(^3\Pi_u)$, we assume that it has the same cross section as a deuterium atom in the 2s state (see Appendix A), but does not undergo radiative decay. We treat charge exchange as a non-trapping attenuation process, since the beam particle replaces a plasma ion which is neutralized and ejected at some random angle. Finally, we note that at the energies considered here, molecular trapping results mainly in the formation of D_2^+ rather than D^+. The trapped D_2^+ will subsequently dissociate or ionize due to collisions with the ions and electrons in the plasma; dissociation is the more probable process [16]. We will not consider the details of these processes here, but in most cases the neutral atom will escape from the plasma following the dissociation of a D_2^+ ion. Sample values of the cross sections relevant to our calculations are given in the first three columns of Table I [17-20].

To illustrate the difference in trapping of various incident species we first consider the idealized case in which the incident beam is composed entirely of either ground-state D(1s) atoms, ground-state $D_2(^1\Sigma_g)$ molecules, or excited $D_2(^3\Pi_u)$ molecules. In this case, the intensity of a beam with velocity v_0, passing through a plasma of length L, density $n_i = n_e = n$, and electron temperature T_e is given by

$$I = I_0 \exp[-(\sigma_i^+ v_0 + \sigma_i^- v_e + \sigma_{cx} v_0) nL/v_0] \qquad (1)$$

where I_0 is the initial intensity, $v_e = \sqrt{2T_e/m_e}$, and the cross sections are as defined in Table I. The fraction of the beam that contributes an ion to the plasma is then

$$f = \frac{\sigma_i^+ + (v_e/v_0)\sigma_i^-}{\sigma_i^+ + \sigma_{cx} + (v_e/v_0)\sigma_i^-}\left\{\exp[-(\sigma_i^+ + \sigma_{cx} + (v_e/v_0)\sigma_i^-)nL]\right\} \quad (2)$$

The solutions to this equation for the three types of incident beams at 10 keV/nucleon are shown in Fig. 5 for three different electron temperatures (20, 100, and 1000 eV). It can be seen from Fig.5 that there is little difference in trapping efficiency between D(1s) and $D_2(^1\Sigma_g)$ beams, but that trapping is enhanced (especially for low T_e) with a $D_2(^3\Pi_u)$ beam.

The preceding calculation serves to illustrate the increased trapping that could be achieved with a pure $D_2(^3\Pi_u)$ beam. We have shown in Sect. 2, however, that the production of $D_2(^3\Pi_u)$ beams in a Mg target is accompanied by large fractions of ground-state atoms and molecules. The fractions of D, D_2, and $D_2(^3\Pi_u)$ that are produced in a Mg neutralizer optimized for maximum $D_2(^3\Pi_u)$ output for an incident beam of 40-keV D_2^+ ions are listed in the fourth column of Table I. The products of the fractions and the cross sections, $f[\sigma_i^+ + (v_e/v_0)\sigma_i^-]$, give an indication of the relative trapping contributions (column 5). We see that even though the neutralizer is optimized for $^3\Pi_u$ output, the abundance of D atoms tends to mask the $^3\Pi_u$ contribution.

Finally, we know from the Phoenix [21] and Baseball [22] experiments and from theoretical predictions by Hiskes [7] that Lorentz ionization and inverted cascading of highly excited states accounts for most of the trapping at line densities below 10^{12} cm^{-2}. To include highly excited states in our trapping estimate we have used a modified form of a computer code[2] in which the coupled differential equations that describe the population of each species and excited level in the beam are integrated numerically.

The following processes and assumptions (in addition to those mentioned at the beginning of this section) were included in the calculation (specific details are given in Appendix B):

1. A pure D^+ or D_2^+ beam is converted to a neutral beam in a Mg-vapor neutralizer of appropriate thickness to give optimum trapping.[3] When the incident beam is D_2^+, the resulting neutral beam contains ground-state D and D_2, $D_2(^3\Pi_u)$, and highly excited D and D_2. The trapping fraction is defined as the number of ions trapped in the plasma per ion (D^+ or D_2^+) incident on the neutralizer.

2. The excited atoms or molecules undergo radiative decay in a 200-cm flight path between the neutralizer and plasma. Excited D_2 molecules (except $^3\Pi_u$) are assumed to have the same lifetimes as excited D atoms. Since angular-momentum substate distributions are unknown, a statistical distribution is assumed. Statistically averaged lifetimes for decay from quantum level n to each lower level n' are used.

3. The plasma is contained in a magnetic field that will Lorentz-ionize all quantum levels of D and D_2 with $n \geq 15$ ($B \approx 15$ kG). All of $n = 15$ is trapped; the higher levels are lost in the fringe field.

4. The beam undergoes excitation ($n \rightarrow n + 1$), de-excitation ($n \rightarrow n - 1$), and ionization collisions with the ions and electrons of

the plasma while still undergoing radiative decay. Excitation to $n = 15$ is followed by Lorentz trapping (inverted cascading). Cross sections for excited levels of D_2 are taken to be the same as for excited D. The cross sections used for all collisional processes (both H^+ and e^- impact) are electron cross sections except for ground-state and $^3\Pi_u$ ionization by H^+. For electron collisions the cross sections are evaluated at the electron velocity corresponding to the electron temperature. For proton collisions the cross sections are evaluated at the velocity of the incoming neutrals.

The results of this calculation are given in Fig. 6, where we show the trapped fraction vs plasma line density for an injection energy of 10 keV/nucleon and a plasma electron temperature of 100 eV. Because of the finite lifetimes of excited atoms and molecules we have chosen a specific plasma dimension along the injected beam, namely 10 cm, but the results are not sensitive to this dimension for line densities $\int ndl < 10^{14}$ cm^{-2}. For a D^+ beam (dashed lines in Fig. 6), the trapped fraction is the number of D^+ ionized in the plasma per primary D^+ incident on the neutralizer; for D_2^+ (solid lines), the trapped fraction is the number of D^+ and D_2^+ produced in the plasma per primary D_2^+ incident on the neutralizer. The heavy lines indicate the total trapping, which has contributions from direct Lorentz ionization, cascading, and collisional ionization. The thin lines in Fig. 6 give a breakdown of the various contributions: Curves A give the results for collisional ionization of only the ground-sate and $^3\Pi_u$ components [D(1s) or D(1s) + $D_2(^1\Sigma_g)$ + $D_2(^3\Pi_u)$] of the beams. Curves B give the results for collision-induced trapping of all excited states (ignoring the contribution of direct Lorentz ionization).

We see from Fig. 6 that at low plasma line densities ($\lesssim 10^{13}$ cm^{-2}), beams produced by D^+ ions incident on a Mg vapor neutralizer are trapped more efficiently. This is because a greater yield of highly excited D atoms can be obtained with a primary beam of D^+ (see Appendix B). As the plasma density is increased the reservoir of highly excited states is depleted, and for line densities greater than 10^{13} cm^{-2} a $D_2{}^+$ beam incident on a Mg neutralizer shows some advantage. In this example the advantages due to D^+ or $D_2{}^+$ primary beams are not greater than a factor of 2.

A matter of as much importance as the total fraction of a beam that is trapped is the position in the plasma at which trapping occurs. In Fig. 7 we show, as a function of distance into a uniform plasma, the differential trapping of 20-keV/deuteron beams prepared by adjusting the neutralizer thickness so as to maximize the total ion trapping at the indicated line densities.[3] Similar curves are shown in Fig. 8 for the case that the radial variation of plasma density is parabolic. In these figures the neutral particles enter the plasma from the left. (The integrals of the curves in either Fig. 7 or Fig. 8 correspond to points on the curves labeled B in Fig. 6.) The depletion of excited atoms and molecules as the beams traverse the plasma accounts for most of the left-right asymmetry.

Finally, we show the effect of azimuthal averaging of the trapping curves of Figs. 7 and 8, assuming that ions trapped at radii ±r will drift azimuthally to fill a cylindrical shell. The example shown in

Fig. 9 is for $\int ndl = 10^{13}\ \mathrm{cm}^{-2}$. We see that the density of trapped beam particles near the axis is somewhat larger if the initial beam is D_2^+ rather than D^+.

4. DISCUSSION

We have shown (Fig. 5) that the injection of pure beams of $D_2(^3\Pi_u)$ molecules could, for low energies and plasma electron temperatures, lead to trapping that is many times more efficient that that calculated for beams of ground-state atoms. However, for the maximum experimental $^3\Pi_u$ yield that we report here (6.5% of an incident beam of 43-keV D_2^+ ions), the difference between molecular and atomic beams is less dramatic. In the examples that we have calculated, the total trapping efficiency of beams of D_2^+ ions can be about twice that which could be obtained with a beam of D^+ ions. The relative merits of the different radial trapping distributions of neutral beams produced by D^+ or D_2^+ neutralized in Mg vapor (Figs. 7-9) are difficult to comment on without knowing details of the plasma processes important to a specific experiment.

Beams containing $D_2(^3\Pi_u)$ molecules may, in fact, show more advantage that is suggested above. First, we note from Fig. 3 that the fraction of a D_2^+ beam that can be converted to $D_2(^3\Pi_u)$ molecules rises rapidly with decreasing energy. Therefore, the neutral beam may have appreciably more $D_2(^3\Pi_u)$ molecules at energies below our lowest energy of 43 keV. Second, the passage of an intense ion beam through a neutralizer may produce a sufficient degree of ionization (say 1%) to destroy most of the highly excited levels of an atomic beam [23]. In this case, curves A of Fig. 6 would represent the experimental situation over a broader range of plasma line densities.

The differential trapping vs radius (Figs. 7 and 8) would be quite different, having approximately the shape of the plasma density distribution (uniform or parabolic), with the D_2^+ curves always lying above D^+. The capture averaged over cylindrical shells (Fig. 9) would not be affected appreciably at small radii, but all curves would decrease monotonically at large radii.

In summary, our sample calculations show that if D^+ and D_2^+ ion currents could be produced with equal ease, then conversion of D_2^+ ions in Mg-vapor neutralizers optimized for $D_2(^3\Pi_u)$ production would offer some advantages with respect to total trapping and, at intermediate target-plasma densities, maximization of trapping near the center of the plasma. If, for some reason, the excited states of D atoms should be depleted before reaching the plasma, the advantages would be enhanced.

ACKNOWLEDGMENT

We thank Dr. John R. Hiskes of the Lawrence Livermore Laboratory for suggesting this investigation and for many helpful discussions.

APPENDICES

A. Ionization of $D_2(^3\Pi_u)$

We do not know of any cross-section measurements or calculations for the ionization of $D_2(^3\Pi_u)$ by electron- or proton-impact. We assume that the ionization cross section for $D_2(^3\Pi_u)$ is the same as for an H atom in the n = 2 level, and we use the following arguments to justify this assumption.

At infinite nuclear separation the $D_2(^3\Pi_u)$ molecule is made up of a D(1s) and D(2p) atom; very roughly, then, the $^3\Pi_u$ molecule can be pictured as a D_2^+ ion at the core orbited by a 2p electron, and the ionization cross section should be similar to that for a D atom in the 2p state. (We note that the binding energies of both D(n = 2) and $D_2(^3\Pi_u)$ are about 3.4 eV.) Furthermore, except for hyperfine structure, the D atom and H atom have the same electronic structure, hence the same cross sections.

The cross section for ionization of H(2s) by electron impact has been measured by Dixon and Harrison [24]. Born approximation calculations by Omidvar [25] show that the ionization cross section is not sensitive to the angular momentum state; we therefore use the H(2s) cross sections for the $D_2(^3\Pi_u)$ molecule. To estimate the cross section for proton impact we evaluated Gryzinski's [26] formulas for both proton- and electron-impact. As expected, these two cross sections converge at high velocities; however, the Gryzinski electron-impact cross section is about 1.5 times larger than the cross sections measured by Dixon and Harrison. We therefore divided the Gryzinski proton-impact cross section by 1.5. The normalized Gryzinski cross sections and those of Harrison are shown in Fig. A1.

B. Input for Numerical Calculations

In this appendix we give more detailed information on the values used as input for the calculations described in Sect. 3. The numbered sections coincide with the list given in Sect. 3.

1. Available data on yields of highly excited ($n > 2$) D atoms and D_2 molecules from Mg neutralizers are fragmentary and show large discrepancies (see Table BI) [12-14, 27-30]. The data from [13] and [29] (for H and H_2) all come from the same research group, and since we are mainly interested in a comparison of D and D_2, we have chosen their results. Combining these results with the yields given in Sect. II, we obtain the following fractional populations per incident ion:

(a) 20-keV D^+ incident on Mg vapor optimized for excited atom production ($\sim 5 \times 10^{14}$ Mg atoms/cm^2):

$D(1s) = 0.6$

$D(n) = 1.0\ n^{-3}$

(b) 20-keV D^+ incident on thick Mg-vapor target ($\sim 10^{16}$ Mg atoms/cm^2):

$D(1s) = 0.92$

$D(n) = 0.1\ n^{-3}$

(c) 40-keV D_2^+ incident on Mg vapor optimized for $D_2(^3\Pi_u)$ production ($\sim 7 \times 10^{14}$ Mg atoms/cm^2):

$D(1s) = 1.07$

$D(n) = 0.4\ n^{-3}$

$D_2(^1\Sigma_g) = 0.155$

$D_2(^3\Pi_u) = 0.065$

$D_2(n) = 0.1\ n^{-3}$

(d) 40-keV D_2^+ incident on thick Mg-vapor target ($\sim 10^{16}$ Mg atoms/cm^2):

$D(1s) = 1.84$

$D(n) = 0.1\ n^{-3}$

$D_2(^1\Sigma_g) = 0$

$D_2(^3\Pi_u) = 0$

$D_2(n) = 0$

2. For radiative decay of the excited atoms we used statistical averages,

$$A(n \rightarrow n') = \sum_{\ell,\ell'} (2\ell + 1)n^{-2}A(n\ell \rightarrow n'\ell')$$

of the transition probabilities evaluated by Hiskes, Tarter, and Moody [31]. We remind the reader that statistically averaged transition probabilities are independent of the representation, Stark or field-free, that is used.

3. The electric field required to field-ionize n = 15 was obtained from calculations by Bailey, Hiskes, and Riviere [32].

4. (a) Excitation: For excitation by deuterons we used the theoretical $n \rightarrow n + 1$ cross sections of Saraph [33], evaluated at the equivalent electron energy of 5.5 eV; for excitation by the electrons we used the theoretical $n \rightarrow n + 1$ and $n \rightarrow n + 2$ cross sections of McCoyd and Milford [34]. The Saraph cross sections agree with the low-energy experimental results of Johnson and Hinnov [35] and with the McCoyd and Milford calculations at high energies.

(b) De-excitation: De-excitation cross sections were obtained from the relationship

$$\sigma_{n+1,n} = \left(\frac{n}{n+1}\right)^2 \sigma_{n,n+1}$$

(c) Ionization: The cross section for ionization of $n = 2$ is discussed in Appendix A. For $n > 2$ we applied the scaling law suggested by Percival [36] ($n^4 \sigma_{H(n)\to H^+}$ vs $n^2 E$ is a universal curve) to the Born calculations of Omidvar [25] for $n = 2$ to 5.

FOOTNOTES

1. In the experiment both H_2^+ and D_2^+ were used. The yields are the same at equal velocities, and in this paper we report all results in terms of the equivalent D_2^+ energy.
2. The code was developed for H-atom trapping by K. H. Berkner and A. C. Riviere in 1966 at the UKAEA Culham Laboratory.
3. Calculations were performed for beams produced by either thick targets of magnesium or magnesium neutralizers optimized for excited-atom or excited-molecule yields. The results for the neutralizer thickness giving the greater trapping were used. For D^+ beams, thick targets were used for plasma line densities $\geq 10^{14}$ cm^{-2}; for D_2^+ beams, line densities $\geq 10^{15}$ cm^{-2}.

REFERENCES

[1] BARNETT, C. F., RAY, J. A., THOMPSON, J. C., Atomic and Molecular Collision Cross Sections of Interest in Controlled Thermonuclear Research, Oak Ridge National Laboratory Report ORNL-3113 Revised (Aug. 1964), unpublished.

[2] For trapping of H beams see, e.g., RIVIERE, A. C., Nucl. Fusion 11 (1971) 363.

[3] HISKES, J. R., Lawrence Livermore Laboratory Report UCRL-73632 (1971), unpublished.

[4] See, e.g., SPITZER, L., et al., NYO-6047 (1954) 196, unpublished; GROLNICK, S. L., Solid Deuterium Evaporation in a Fusion Plasma, Ph. D. Thesis, Columbia University (1972), unpublished.

[5] HISKES, J. R., Nucl. Fusion 2 (1962) 38.

[6] SWEETMAN, D. R., Nucl. Fusion Suppl., Part 1 (1962) 279.

[7] HISKES, J. R., Phys. Rev. Letters 10 (1963) 102.

[8] HISKES, J. R., Bull. Am. Phys. Soc. 13 (1968) 308.

[9] FREIS, R. P., HISKES, J. R., Phys. Rev. A 2 (1970) 573; HISKES, J. R., Phys. Rev. 180 (1969) 146.

[10] MORGAN, T. J., BERKNER, K. H., PYLE, R. V., Phys. Rev. A 5 (1972) 1591.

[11] RIVIERE, A. C., V ICPEAC, Leningrad (1967) 15.

[12] KINGDON, J., PAYNE, M., RIVIERE, A. C., UKAEA Culham Laboratory Reports CLM-PR10 (1967) 56, unpublished, and CLM-PR11 (1968) B23, unpublished.

[13] SOLOV'EV, E. S., IL'IN, R. N., OPARIN, V. A., FEDORENKO, N. V., Zh. Eksp. Teor. Fiz. 53 (1965) 1933. [English Transl.: Sov. Phys.-JETP 26 (1968) 1097.]

[14] FUTCH, A. H., MOSES, K. G., Bull. Am. Phys. Soc. <u>11</u> (1966) 344, and private communication.

[15] BERKNER, K. H., PYLE, R. V., STEARNS, J. W., Phys. Rev. <u>178</u> (1969) 248.

[16] ALSMILLER, R. G., JR., Oak Ridge National Laboratory Report ORNL-3232 (1962), unpublished.

[17] McDANIEL, E. W., Collision Phenomena in Ionized Gases, John Wiley and Sons, New York (1966).

[18] Bates, D. R., Ed., Atomic and Molecular Processes, Academic Press, New York (1962), p. 751.

[19] BOYD, T. J. M., DALGARNO, A., Proc. Phys. Soc. (London) <u>72</u> (1958) 694.

[20] KIEFFER, L. J., Atomic Data <u>1</u> (1969) 20.

[21] THOMPSON, E., CORDEY, J. G., SWEETMAN, D. R., in Plasma Physics and Controlled Nuclear Fusion Research 1971, IAEA, Vienna (1971), Vol. 2, p. 689.

[22] DAMM, C. C., FOOTE, J. H., FUTCH, A. H., GOODMAN, R. K., GORDON, F. J., HAMILTON, G. W., HUNT, A. L., MALLON, R. G., OSHER, J. E., Bull. Am. Phys. Soc. <u>16</u> (1971) 1255; BERKNER, K. H., COOPER, W. S., DAMM, C. C., EHLERS, K. W., FUTCH, A. H., HAMILTON, G. W., OSHER, J. E., PYLE, R. V., in Plasma Physics and Controlled Nuclear Fusion Research 1971, IAEA, Vienna (1971), Vol. 2, p. 707.

[23] BERKNER, K. H., KING, I. I., RIVIERE, A. C., Nucl. Fusion <u>7</u> (1967) 115.

[24] DIXON, A. J., HARRISON, M. F. A., VII ICPEAC, Amsterdam (1971), p. 892.

[25] OMIDVAR, K., Phys. Rev. 140 (1965) A26.

[26] GRYZINSKI, M., Phys. Rev. 138 (1965) A336.

[27] FUTCH, A. H., MOSES, K. G., VI ICPEAC, Leningrad (1967) p. 12; more details are given in Lawrence Livermore Laboratory Report UCRL-70251 Summary (1967), unpublished.

[28] McFARLAND, R. H., FUTCH, A. H., JR., Phys. Rev. A 2 (1970) 1795.

[29] SOLOV'EV, E. S., IL'IN, R. N., OPARIN, V. A., FEDORENKO, N. V., Zh. Eksp. Teor. Fiz. 53 (1967) 1933. [English transl.: Sov. Phys.-JETP 26 (1968) 1097.]

[30] BERKNER, K. H., COOPER, W. S., KAPLAN, S. N., PYLE, R. V., Phys. Rev. 182 (1969) 103.

[31] HISKES, J. R., TARTER, C. B., MOODY, D. A., Phys. Rev. 133 (1964) A424; numerical values were taken from HISKES, J. R., TARTER, C. B., Lawrence Livermore Laboratory Report UCRL-7088 Rev. I (1964), unpublished.

[32] BAILEY, D. S., HISKES, J. R., RIVIERE, A. C., Nucl. Fusion 5 (1965) 41.

[33] SARAPH, H. E., Proc. Phys. Soc. (London) 83 (1964) 763.

[34] McCOYD, G. C., MILFORD, S. N., Phys. Rev. 130 (1963) 206.

[35] JOHNSON, L. C., HINNOV, E., Phys. Rev. 187 (1969) 143.

[36] PERCIVAL, I., Nucl. Fusion 6 (1966) 182.

TABLE I. A comparison of parameters pertinent to a trapping calculation for 10-keV/nucleon D(1s), $D_2(^1\Sigma_g)$, and $D_2(^3\Pi_u)$ impinging upon a plasma with electron temperature $T_e = 100$ eV. σ_{cx}: charge exchange cross section; σ_i^-: cross section for ionization by 100-eV electrons; σ_i^+: cross section for ionization by 20-keV D^+; f: number of D(1s), $D_2(^1\Sigma_g)$, or $D_2(^3\Pi_u)$ per D_2^+ ion incident on a Mg neutralizer optimized for $D_2(^3\Pi_u)$ production. All cross sections are in units of 10^{-16} cm^2. The last column, $f[\sigma_i^+ + (v_e/v_0)\sigma_i^-]$, gives an indication of the relative trapping contribution of each component of the beam.

	σ_{cx}	σ_i^-	σ_i^+	f	$f[\sigma_i^+ + (v_e/v_0)\sigma_i^-]$
D(1s)	10^a	0.6^d	1.0^g	1.07	3.83
$D_2(^1\Sigma_g)$	8^b	1.0^e	0.7^h	0.155	0.77
$D_2(^3\Pi_u)$	8^c	2.7^f	17^f	0.065	1.86

---

a) Ref. [17], p. 253.

b) Ref. [18], p. 751.

c) Guided by calculations for $H^+ + H(2s,2p) \rightarrow H(2s,2p) + H^+$ by Boyd and Dalgarno [19], extrapolated to 10 keV, we assume that $D^+ + D_2(^3\Pi_u) \rightarrow D + D_2^+$ has the same cross section as $D^+ + D_2(^1\Sigma_g) \rightarrow D + D_2^+$.

d) Ref. [20], p. 24.

e) Ref. [20], p. 50.

f) See Appendix A.

g) Ref. [17], p. 330.

h) Ref. [17], p. 282.

Table BI. Summary of the data on the production of highly excited, 10 keV/nucleon H^+ and H_2^+ in Mg-vapor neutralizer. The coefficient α_0 is the thin-target value of $\alpha = n^3F_n/F_0$, where F_n is the fraction of the incident beam in the level with principal quantum number n and F_0 is the neutral fraction. The maximum excited-atom fraction is given by $(n^3F_n)_{opt}$.

Incident ion	Excited species	α_0	$(n^3F_n)_{opt}$	n^3F_n (thick target)	Optimum target thickness 10^{14} atoms/cm^2	Neutral fraction at optimum target thickness	Equilibrium neutral fraction $F_{0\infty}$	Reference
10-keV H^+	H^*	1.25	0.53		5	0.6	0.92	Futch, Moses [4,27]
			0.43					Kingdon et al. [12]
		1.3						McFarland, Futch [28]
		1.2	1.0	0.1			0.94	Oparin et al. [29]
		1.2			4	0.55	0.92	Berkner et al. [30]
20-keV H_2^+	H^*	0.06[a]	0.4					Solov'ev et al. [13]
		0.17[a]						Kingdon et al. [12]
20-keV H_2^+	H_2^*	0.095						Solov'ev et al.[13]
40-keV H_2^{+b}	H_2^*	0.26	0.12		3			Solov'ev et al. [13]
		1.5						Kingdon et al. [12]

[a] Extrapolated to 10 keV/nucleon.

[b] Since $(n^3F_n)_{opt}$ is not available for 20 keV H_2^+, we also include 40-keV H_2^+ to indicate its magnitude.

FIGURE LEGENDS

FIG. 1. Fraction of incident D_2^+ ions converted to D_2 molecules vs Mg-vapor thickness. Solid symbols, present work; open symbols, Ref. [12]. x, 30 keV; ●, 40 keV; +, 50 keV; ▲, △, 80 keV; ◆ ;100 keV; ■, 120 keV. The lines through the points are drawn to guide the eye and have no other significance. Representative standard errors are shown.

FIG. 2. The fraction of incident D_2^+ ions that are converted to $D_2(^3\Pi_u)$ molecules vs Mg-vapor thickness. ●, 43 keV; +, 60 keV, ▲, 80 keV. The lines through the points are drawn in to guide the eye and have no other significance.

FIG. 3. Experimental maximum fractions obtained from optimized Mg-vapor targets: ●, maximum fraction of D_2^+ ions converted to D_2 molecules in all states; ◇, maximum fraction of D_2^+ ions converted to $D_2(^3\Pi_u)$ molecules; ▲, maximum fraction of D_2 molecules in $^3\Pi_u$ state.

FIG. 4. The number of D atoms that emerge from a Mg-vapor neutralizer, per incident D_2^+ ion, vs Mg-vapor thickness. Present results: ●, 20-keV D from 40-keV D_2^+; ▲, 40-keV D from 80-keV D_2^+. Equilibrium values: A, Ref. [14], B, Ref. [15]. Solid lines drawn through the present points are extrapolated to equilibrium values by dashed lines.

FIG. 5. Fraction of neutral deuterium beams trapped after traversing a plasma thickness of $\int ndl$ electrons/cm^2 for T_e = 20, 100, and 1000 eV. The curves are for initially pure beams of ground-state atoms (——), ground-state molecules (– –), and excited molecules (---).

FIG. 6. Fraction of 20-keV D^+ (dashed lines) or 40-keV $D_2{}^+$ ions (solid lines) incident on a Mg-vapor neutralizer that produce trapped ions in a plasma with $T_e = 100$ eV vs plasma line density $\int ndl$. The thin lines labeled A represent collisional ionization of ground and $^3\Pi_u$ states, those labeled B are for collision-induced trapping of all excited states, and the heavy lines represent trapping by all processes, including direct Lorentz ionization.

FIG. 7. Differential trapping of 20-keV D^+ and 40-keV $D_2{}^+$ beams, incident on an optimized Mg neutralizer, vs position in a uniform-density, $T_e = 100$ eV, plasma (fraction trapped per cm). Curves for initial D^+ (dashed lines) and $D_2{}^+$ (solid lines) ion beams are shown for four plasma line densities, $\int ndl = 10^{11}$ to 10^{14} electrons/cm^2.

FIG. 8. Same as Fig. 7 except that the plasma density has a parabolic distribution.

FIG. 9. Fractions of initial 20-keV/deuteron D^+ (dashed lines) and $D_2{}^+$ (solid lines) ion beams that are trapped per unit cross sectional area of the plasma at each radius vs radius r. At large radii this is equal to the fraction trapped per unit path length, divided by $2\pi r$. The symbols U and P refer to uniform and parabolic plasma density distributions, both having the same total thickness $\int_{-R}^{R} ndr = 10^{13}$ cm^{-2}.

FIG. A1. Cross sections for the ionization of H(2s) by electrons and protons. The points are the electron-impact cross sections measured by Dixon and Harrison [24]. The curves are calculated from Gryzinski's [26] formulas, normalized to the Dixon and Harrison results by dividing by 1.5: ——, proton impact; ---, electron impact.

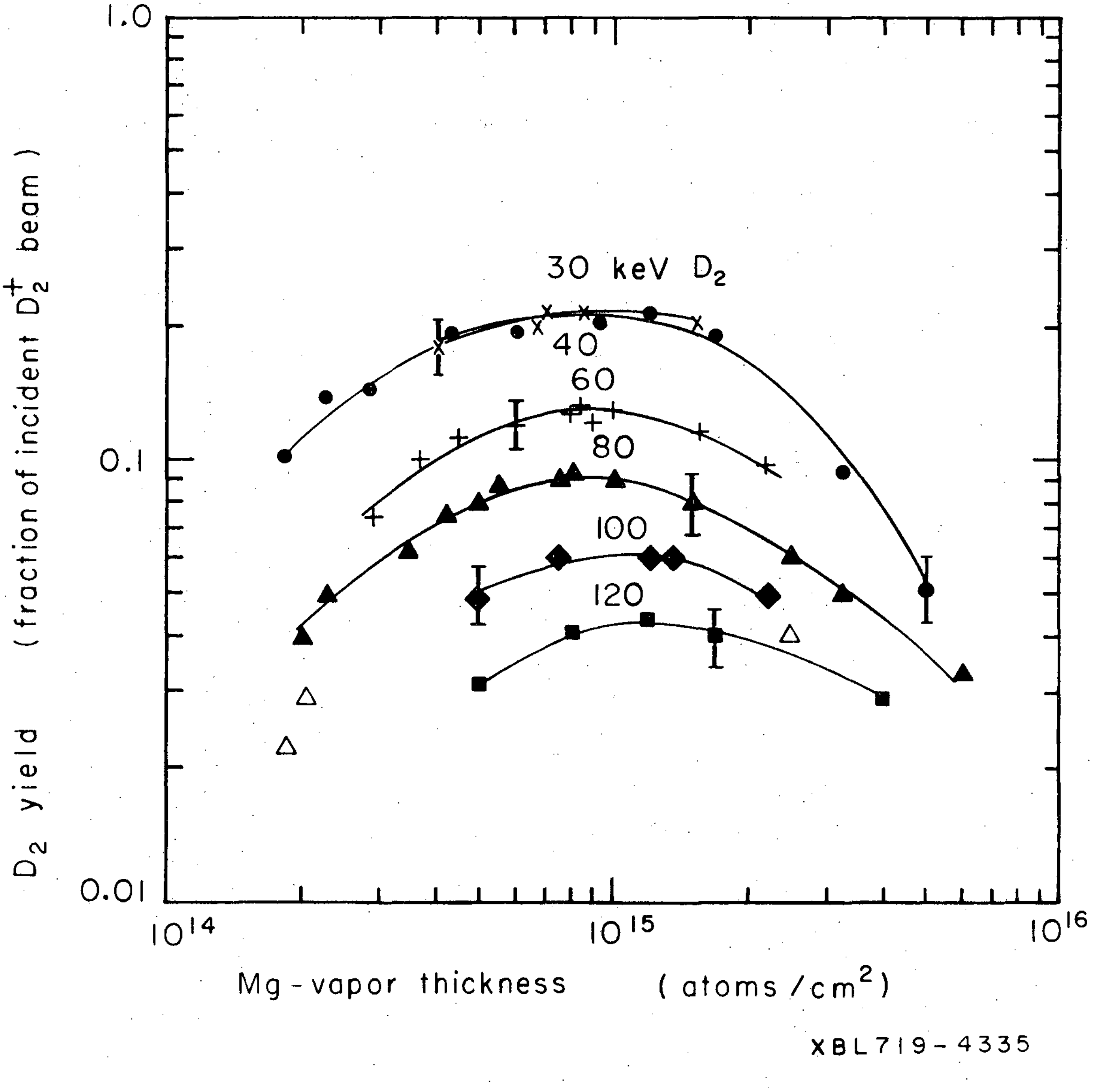
1.0
0.1
0.01
10^{14}
10^{15}
10^{16}
D_2 yield (fraction of incident D_2^+ beam)
Mg-vapor thickness (atoms/cm^2)
30 keV D_2
40
60
80
100
120
XBL719-4335

Fig. 1

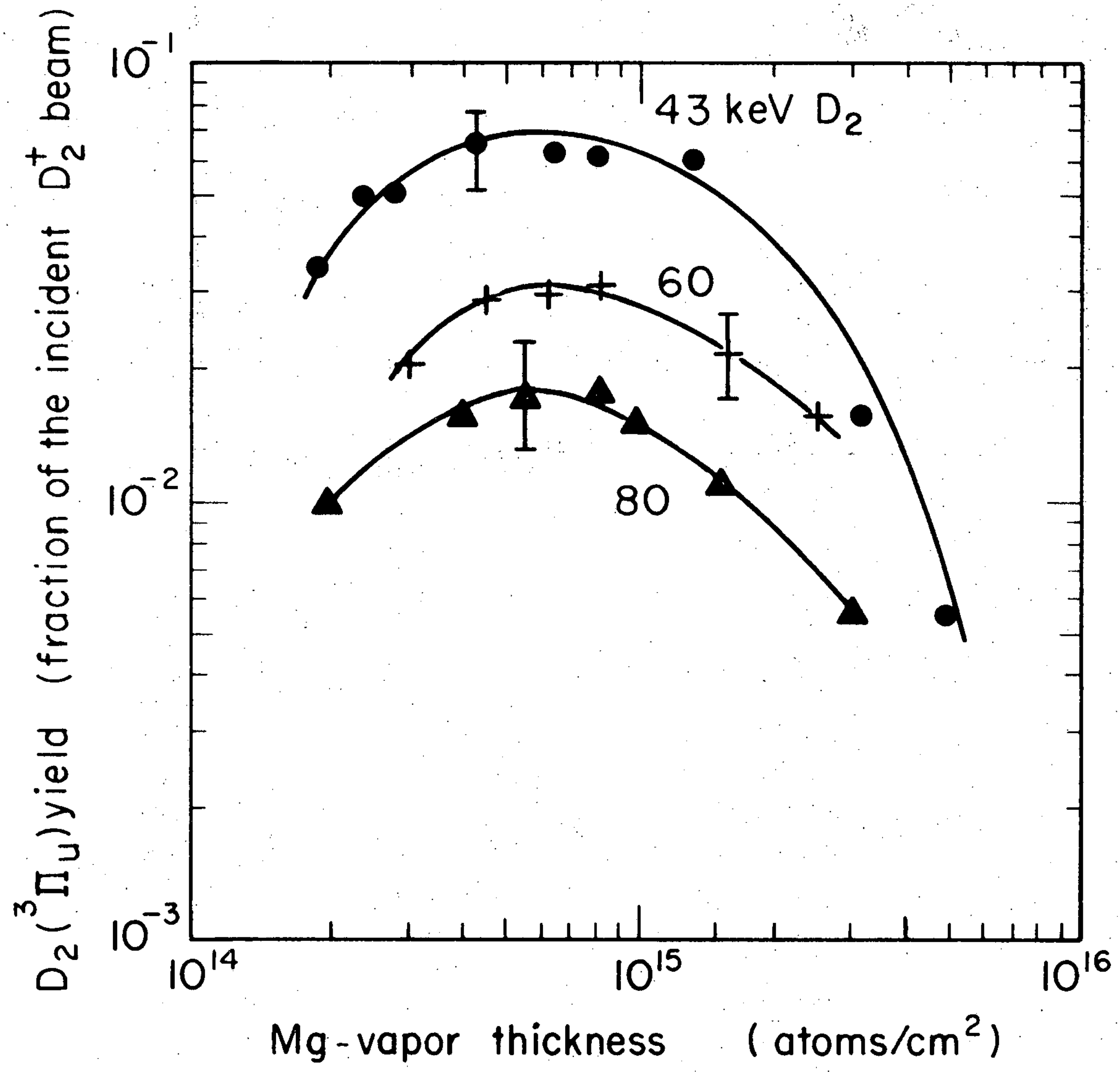

XBL728-3746

Fig. 2

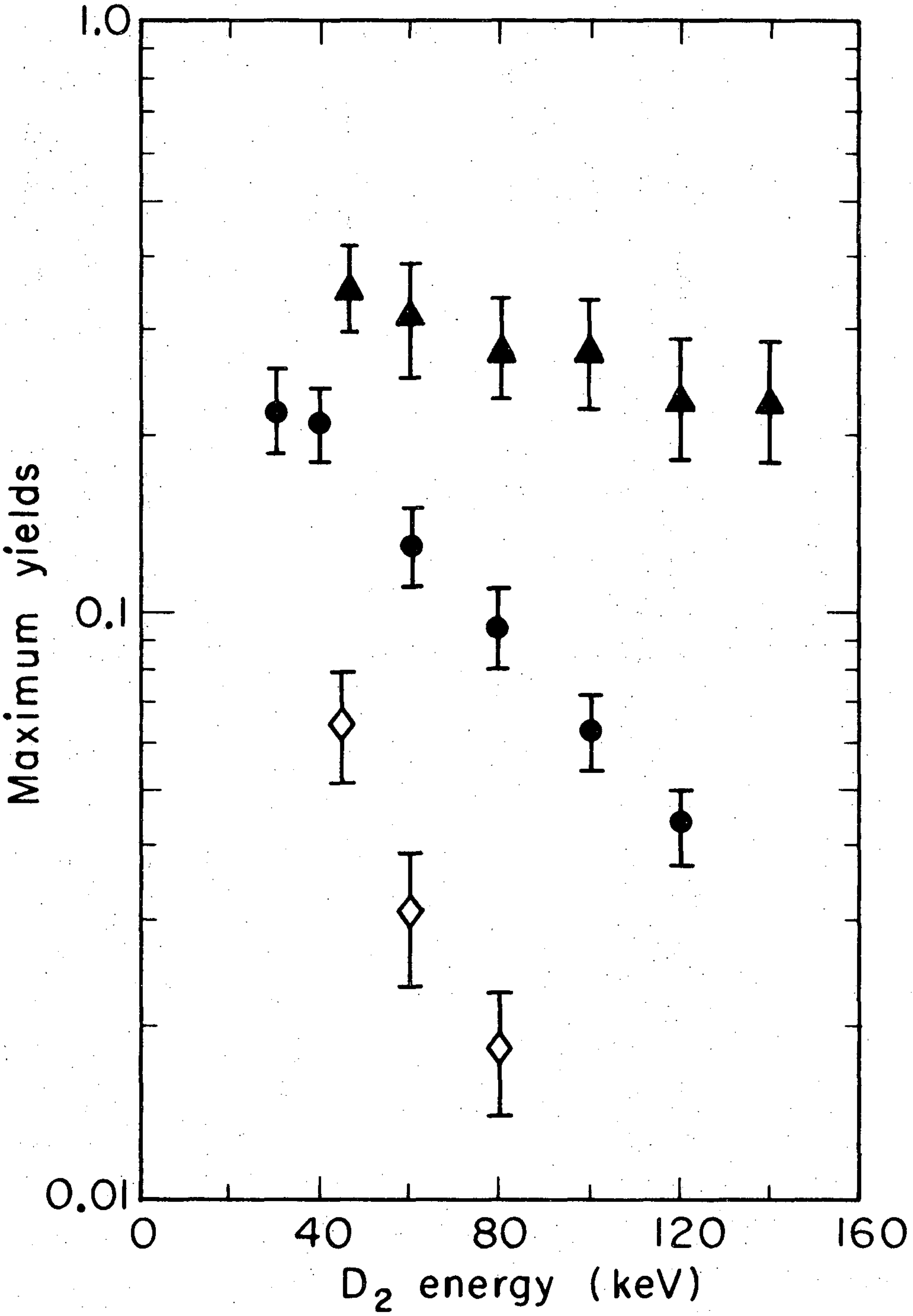

XBL728-3747

Fig. 3

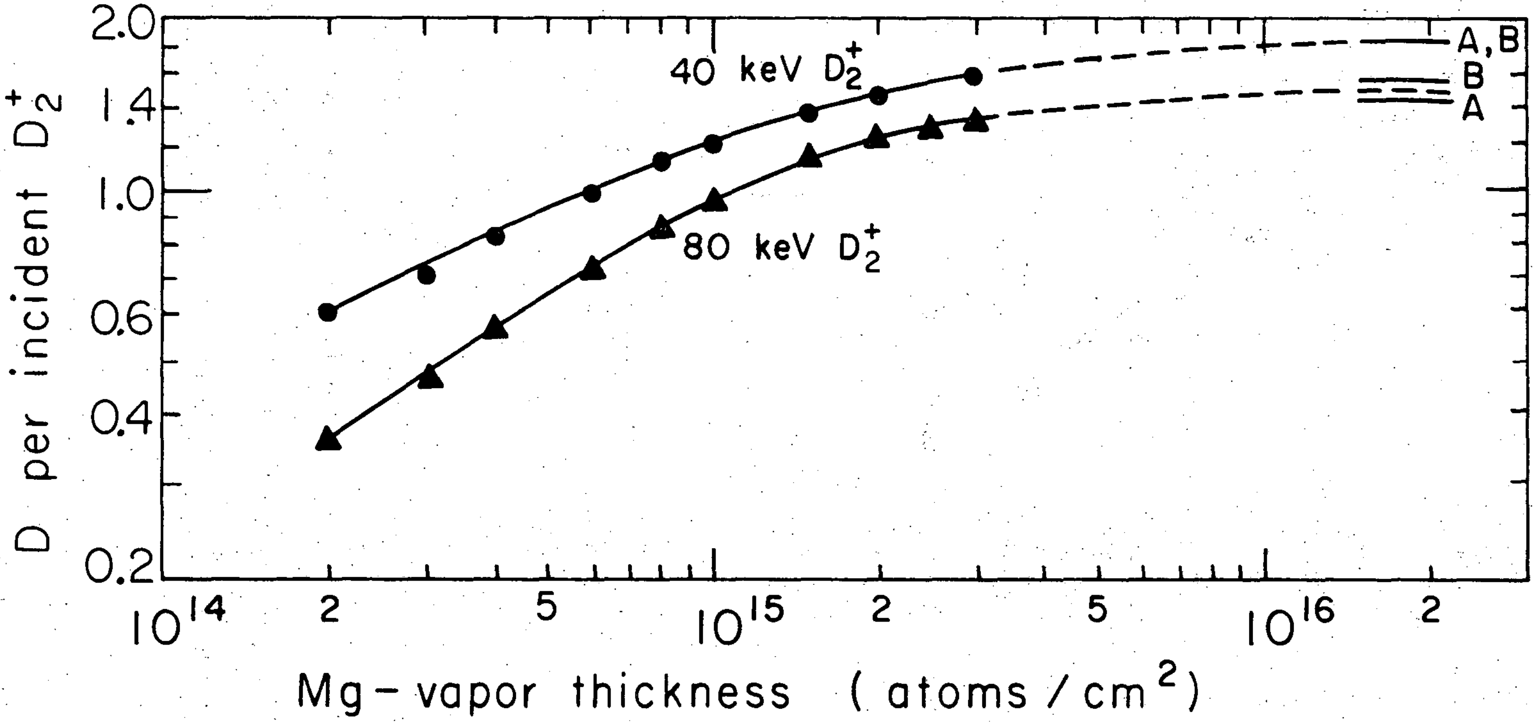

XBL728-3734

Fig. 4

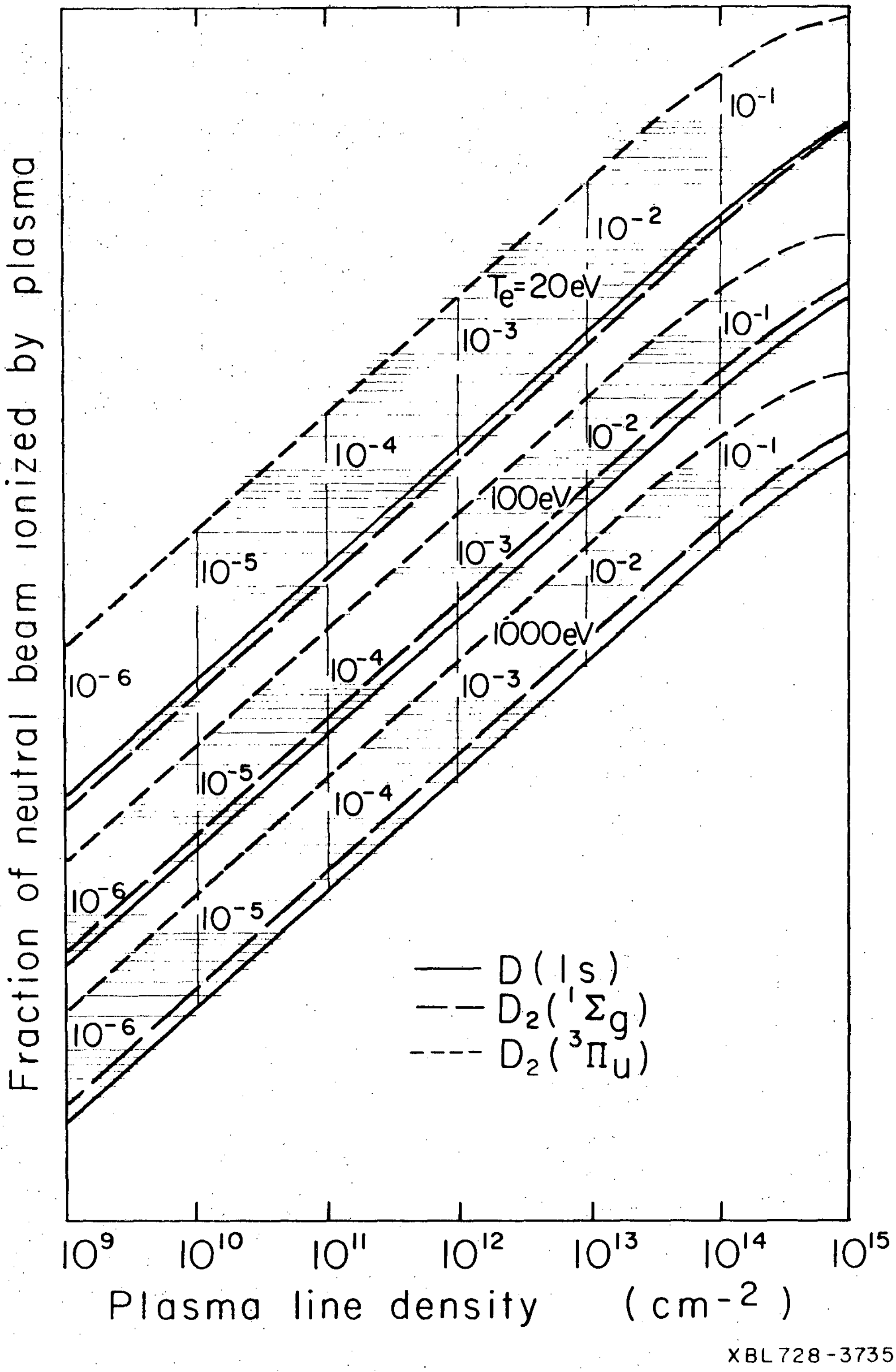
Fraction of neutral beam ionized by plasma
Plasma line density (cm^{-2})
10^{9}
10^{10}
10^{11}
10^{12}
10^{13}
10^{14}
10^{15}
T_e=20eV
100eV
1000eV
10^{-1}
10^{-2}
10^{-3}
10^{-4}
10^{-5}
10^{-6}
D(1s)
$D_2(^1\Sigma_g)$
$D_2(^3\Pi_u)$
XBL 728-3735

Fig. 5

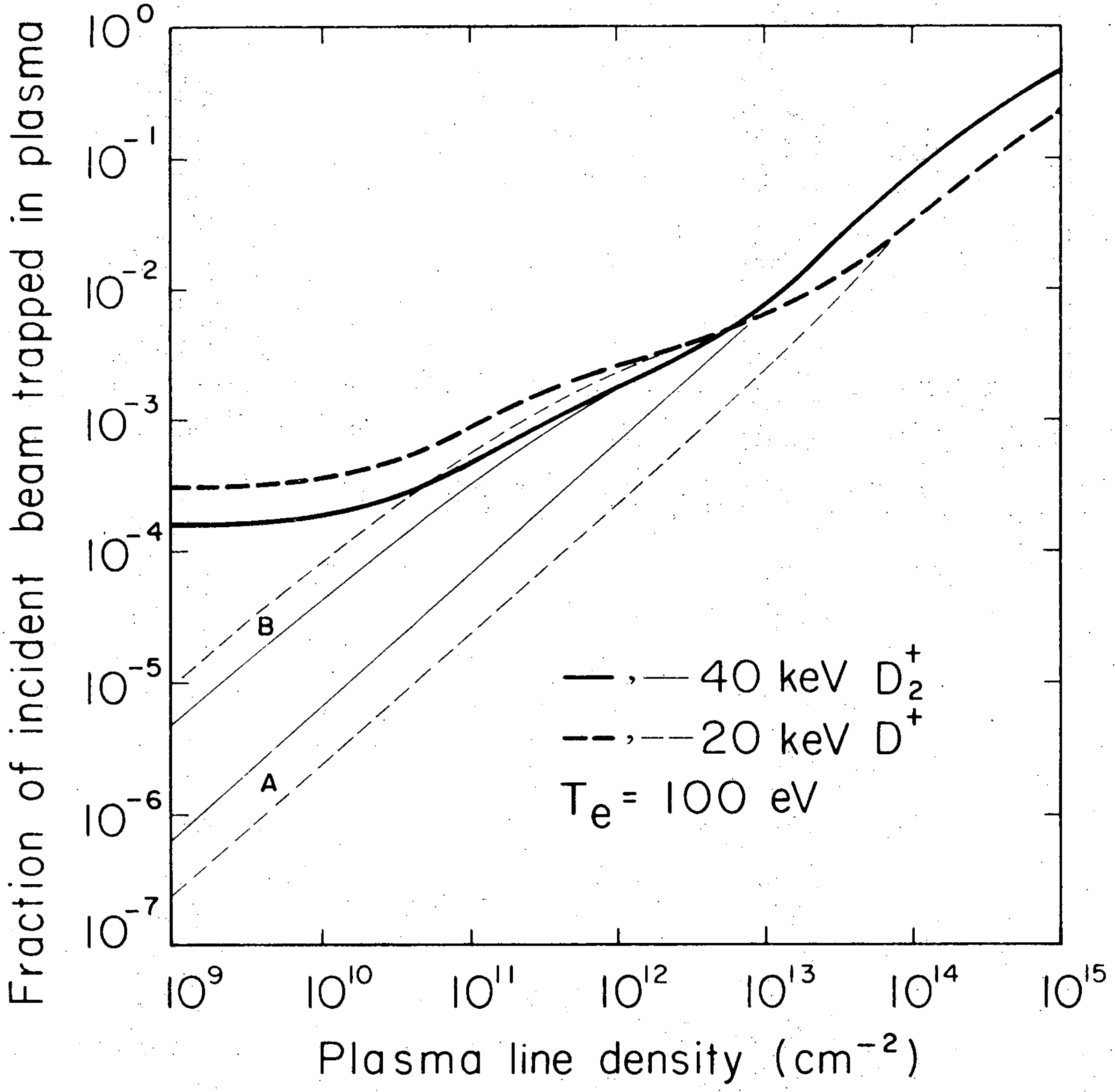

XBL728-3736

Fig. 6

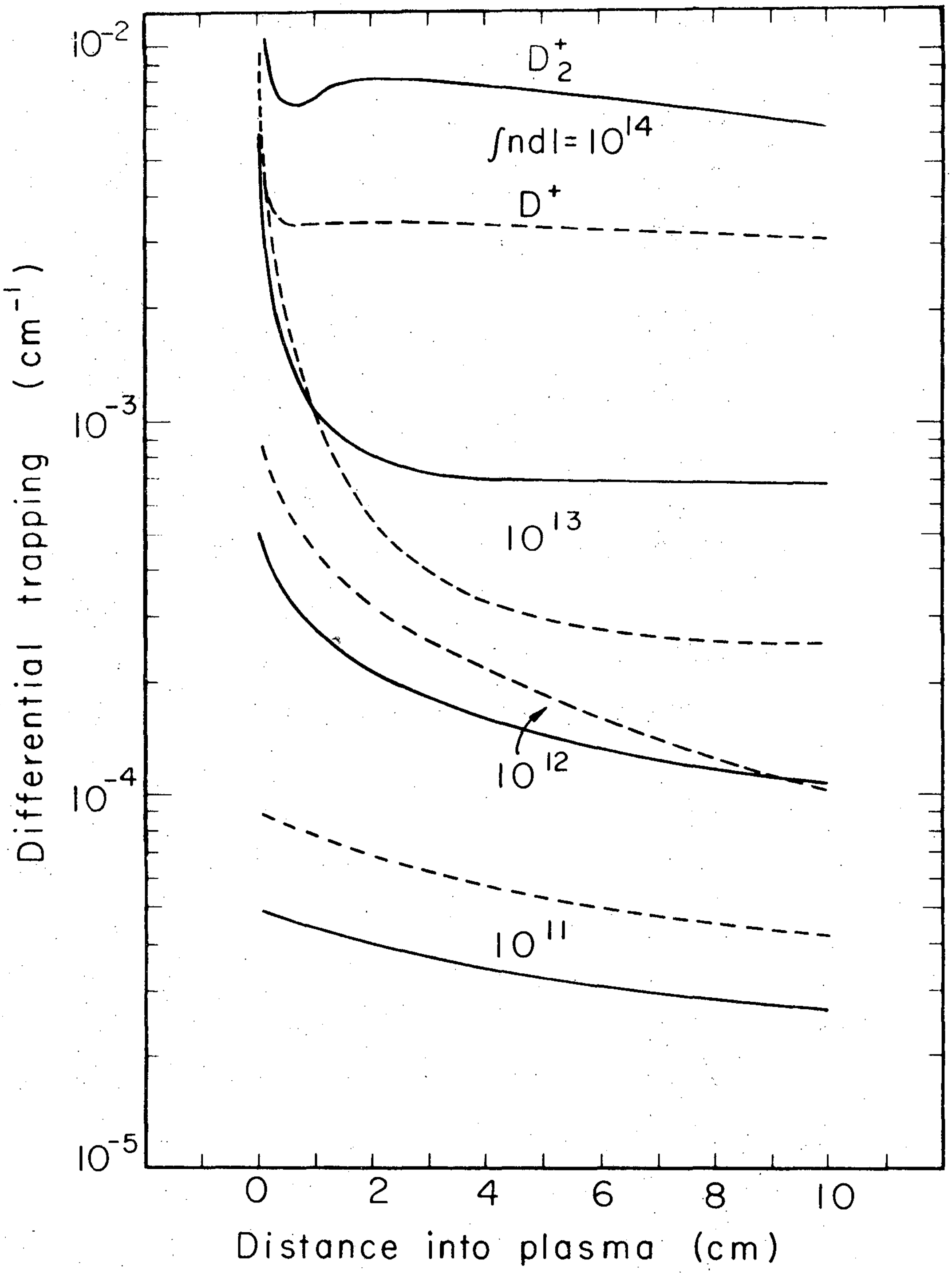

XBL728-3738

Fig. 7

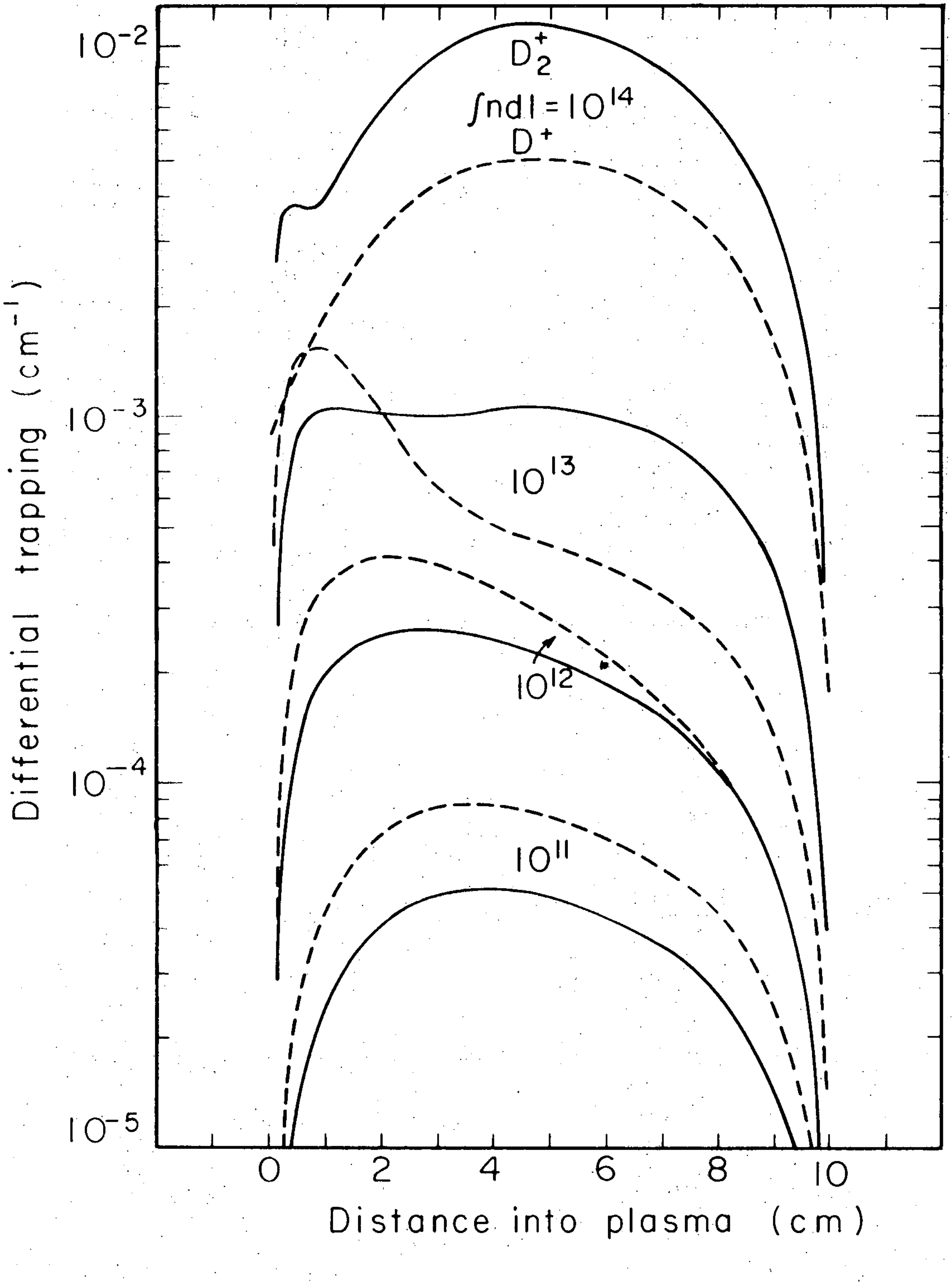

XBL728-3737

Fig. 8

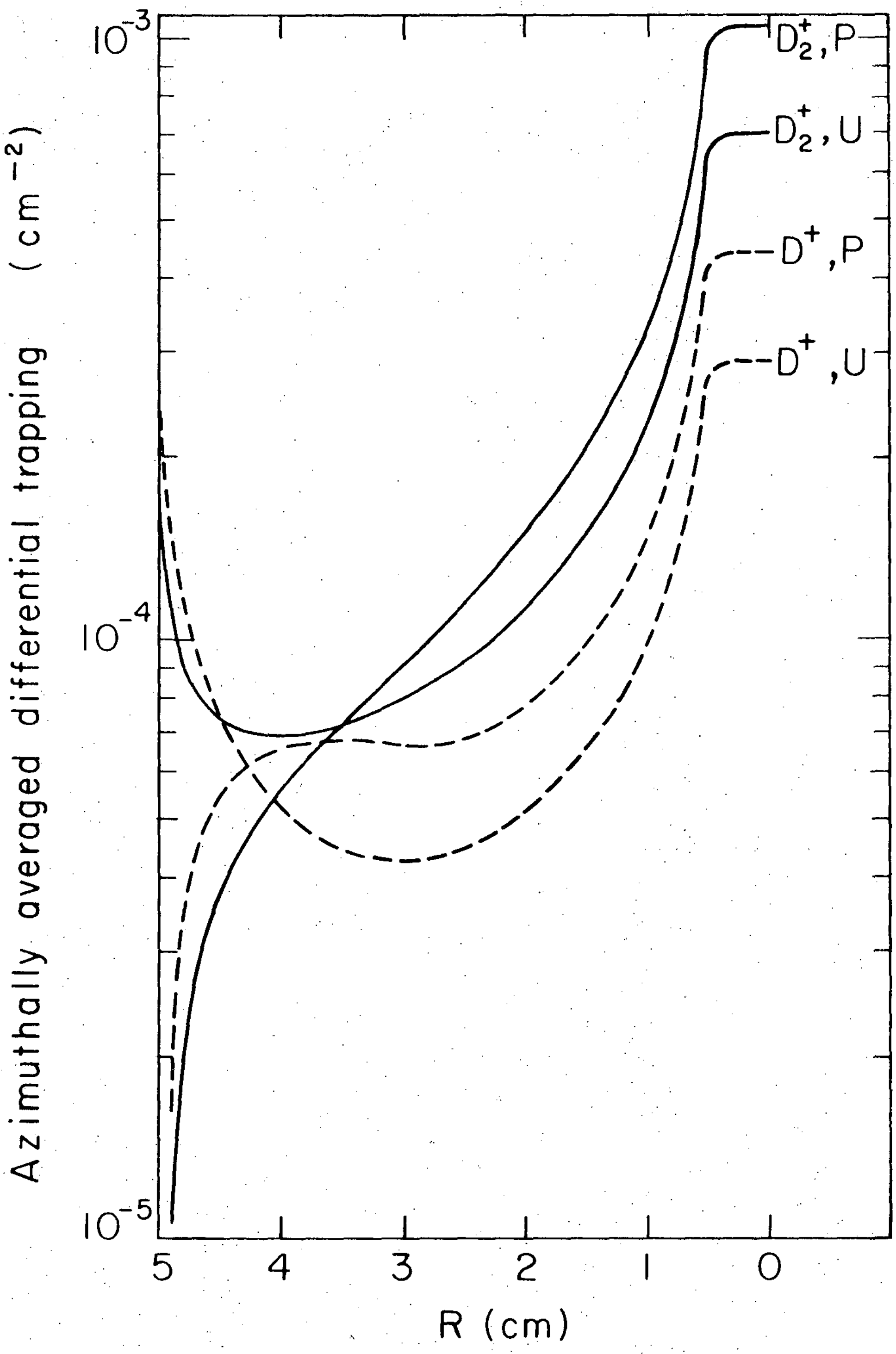

XBL728-3739

Fig. 9

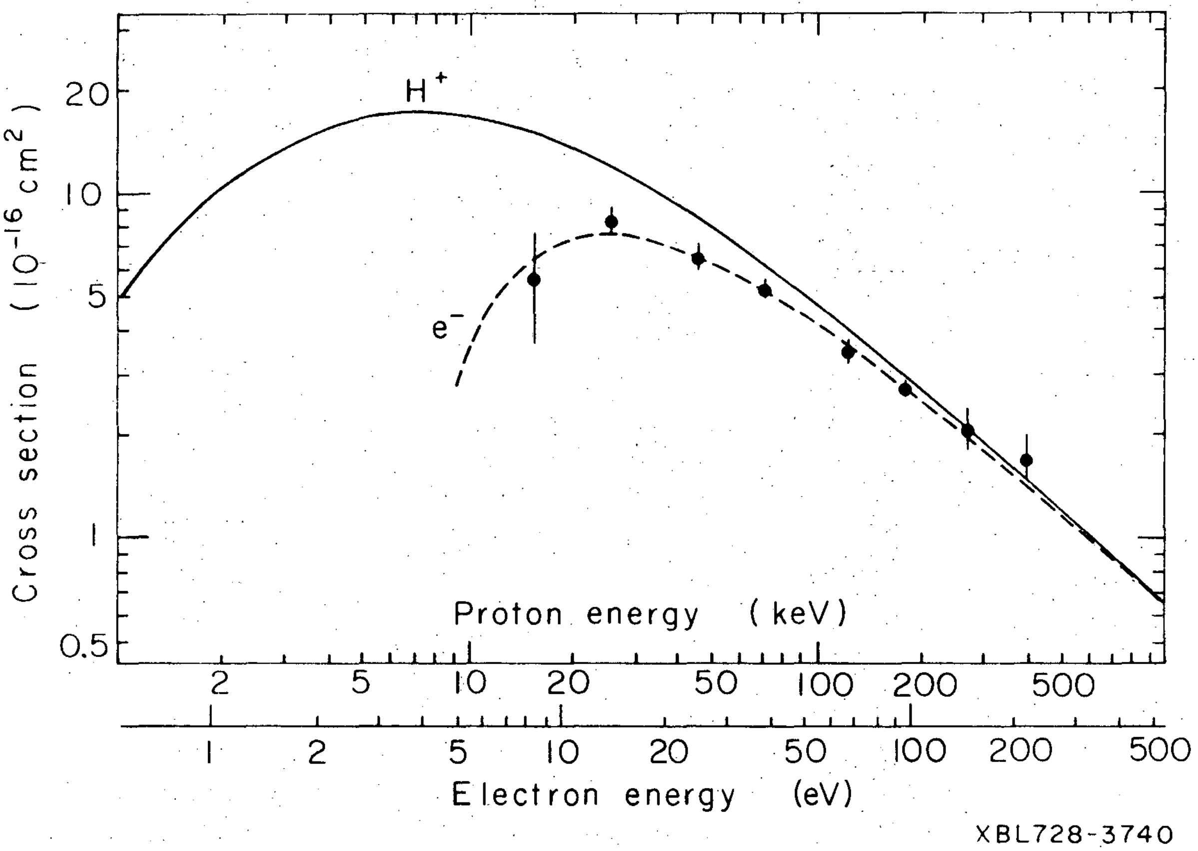
H⁺
e⁻
Cross section (10⁻¹⁶ cm²)
20
10
5
1
0.5
Proton energy (keV)
2
5
10
20
50
100
200
500
1
2
5
10
20
50
100
200
500
Electron energy (eV)
XBL728-3740

Fig. A1

TECHNICAL INFORMATION DIVISION
LAWRENCE BERKELEY LABORATORY
UNIVERSITY OF CALIFORNIA
BERKELEY, CALIFORNIA 94720